Noname manuscript No.
(will be inserted by the editor)

On the computation of area probabilities based on a spatial stochastic model for precipitation cells and precipitation amounts

Björn Kriesche · Antonín Koubek · Zbyněk Pawlas · Viktor Beneš · Reinhold Hess · Volker Schmidt

Received: date / Accepted: date

Abstract A main task of weather services is the issuing of warnings for potentially harmful weather events. Automated warning guidances can be derived, e.g., from statistical post-processing of numerical weather prediction using meteorological observations. These statistical methods commonly estimate the probability of an event (e.g. precipitation) occurring at a fixed location (a point probability). However, there are no operationally applicable techniques for estimating the probability of precipitation occurring anywhere in a geographical region (an area probability). We present an approach to the estimation of area probabilities for the occurrence of precipitation exceeding given thresholds. This approach is based on a spatial stochastic model for precipitation cells and precipitation amounts. The basic modeling component is a non-stationary germ-grain model with circular grains for the representation of precipitation cells. Then, we assign a randomly scaled response function to each precipitation cell and sum these functions up to obtain precipitation amounts. We derive formulas for expectations and variances of point precipitation amounts and use these formulas to compute further model characteristics based on available sequences of point probabilities. Area probabilities for arbitrary areas and thresholds can be estimated by repeated Monte Carlo simulation of the fitted precipitation model. Finally, we verify the proposed model by comparing the generated area probabilities with independent rain gauge adjusted radar data. The novelty of the presented approach is that, for the first time, a widely applicable estimation of area probabilities is possible, which is based solely on predicted point probabilities (i.e., neither precipitation observations nor further input of the forecaster are necessary). Therefore, this method can be applied for operational weather predictions.

Björn Kriesche · Volker Schmidt
Ulm University, Institute of Stochastics, 89069 Ulm, Germany
E-mail: bjoern.kriesche@uni-ulm.de

Antonín Koubek · Zbyněk Pawlas · Viktor Beneš
Charles University in Prague, Faculty of Mathematics and Physics, Department of Probability and Mathematical Statistics, 18675 Prague, Czech Republic

Reinhold Hess
Deutscher Wetterdienst, Research and Development, 63067 Offenbach, Germany

Keywords Area probability · Stochastic model · Occurrence of precipitation · Precipitation amount · Probabilistic weather prediction · Monte Carlo simulation

Acknowledgements The authors gratefully acknowledge the financial supports from the German Academic Exchange Service (DAAD) and the Czech Ministery of Education, project 7AMB14DE006. Antonín Koubek was supported by the grant SVV-2015-260225.

1 Introduction

Meteorological services such as Deutscher Wetterdienst (DWD) are responsible for providing timely, accurate and reliable weather forecasts. A particularly challenging task is the issuing of weather warnings since some weather events (heavy precipitation, strong wind gusts, frozen streets) can cause personal injury and high material damage. At DWD automated warning guidances are derived from a combination of numerical models and statistical post-processing: They commonly provide so-called point probabilities due to the use of meteorological observation systems, e.g. rain gauges, that represent a measurement at a given geographical location (a point). In some cases the consideration of point probabilities is not sufficient for a reasonable weather forecast, e.g., when a critical situation arises if the weather event occurs somewhere in an area (rather than at a fixed point). Examples are given by the area of responsibility of a fire department, which is called into action when there is intense precipitation somewhere within that area or by some warning area of a weather service, which issues a warning of freezing streets in winter if there is some precipitation somewhere within this area (in combination with negative temperature). The probability for a weather event occurring somewhere in an area is called an area probability in this paper. According to this definition, an area probability of some weather event is always larger than or equal to a point probability of the same event for any fixed location within that area.

The exact relationship between point and area probabilities in a general context is still unknown. In [3] and [10] formulas for the computation of area probabilities from point probabilities are given under very restrictive assumptions including circular forecast areas, circular precipitation cells with a known radius and uniformly distributed cell centers. This, however, makes these formulas inappropriate for the automated generation of weather forecasts since model parameters have to be determined by the forecaster. Furthermore, this approach could not be used on a nation-wide scale, where spatial non-stationarity is expected. Alternatively, area probabilities can be estimated based on stochastic models. Recently, a spatial stochastic model for the occurrence of precipitation has been proposed in [8] to specify the relationship between point and area probabilities. In the mentioned approach, the occurrence of precipitation is modeled by a non-stationary germ-grain model, with the circular grains approximating single precipitation cells. The model parameters are computed algorithmically based on available point probabilities and their spatial correlation (which is expected to provide valuable information on the size of precipitation cells). Area probabilities are then computed as coverage probabilities of the suggested germ-grain model.

The consideration of area probabilities for the occurrence of precipitation is not sufficient for the issuing of weather warnings. Weather services are rather interested in area probabilities for the occurrence of precipitation exceeding a certain warning threshold, which cannot be computed using the model suggested in [8]. Thus, the additional modeling of precipitation amounts is necessary. Some approaches to the spatially continuous (off-grid) modeling of precipitation cells including precipitation amounts are given in the literature, see e.g. [11], [16], [17], [18], [19] and the references therein. However, most of the presented approaches are subject to limitations, which make them inappropriate for the automated generation of weather warnings on a nation-wide scale. Such limitations include the assumption of spatial stationarity, constant precipitation amounts per precipitation cell, independence of precipitation cells and precipitation amounts, parameter fitting based on radar observations or the complete absence of model fitting procedures. If applications to real data are provided, then they are mainly focused on a regional scale. Furthermore, none of the mentioned papers deals with the computation of area probabilities. In the last decade, some effort was done to overcome spatial stationarity assumptions using generalized linear models, see e.g. [23], but the considered approaches are not yet applicable for the purpose of spatially continuous modeling. Despite of existing limitations, the mentioned papers still provide a valuable basis for the modeling of precipitation amounts. We focus on some ideas proposed in [16], where precipitation amounts are represented by a stationary shot-noise field based on Poisson or Neyman-Scott point processes. The authors derive several theoretical characteristics of their model and make a comparison for different response functions. Model fitting based on observed data, however, is only described vaguely.

In the present paper, we propose a more robust and less restrictive approach to the modeling of precipitation amounts with the purpose of computing area probabilities for precipitation exceeding an arbitrary threshold. We extend the recently developed non-stationary model for precipitation cells presented in [8] by adding a model for precipitation amounts with spatially varying distributions. All time-dependent model characteristics are computed algorithmically based on available point probabilities (which is a basic requirement for operational weather forecasting). We also show a detailed application of the model to real data on a nation-wide scale. A condensed description presenting an earlier version of the suggested model can be found in [9].

The present paper is organized as follows. In Sect. 2 we briefly outline the computation of point probabilities for precipitation exceeding various thresholds and describe the available data. In Sect. 3 the underlying model for the occurrence of precipitation is recalled, which provides the basis for the newly developed model of precipitation amounts presented in Sect. 4. Sect. 5 deals with the computation of area probabilities for the occurrence of precipitation exceeding a threshold based on the combined model for precipitation cells and amounts. Finally, Sect. 6 provides a verification of results and Sect. 7 concludes the paper.

2 Computation of point probabilities and description of data

In this paper, sequences of point probabilities form the basis for the computation of area probabilities by means of a spatial stochastic model for precipitation cells and precipitation amounts. Therefore, precise point probabilities are critical for the estimation of reliable area probabilities. Point probabilities considered in this paper are determined by DWD in two steps. At first, forecasts of the numerical weather prediction model Globalmodell Europa[1] (GME), see [13], and of the Integrated Forecasting System of the European Centre for Medium-Range Weather Forecasting (IFS/ECMWF) are provided. These forecasts are subject to systematic and random errors, which result from uncertainties in initial weather conditions and inaccuracies in the model specification due to discretization and parametrization. The second step involves Model Output Statistics (MOS), which is a statistical post-processing procedure based on historical information from about 3000 synoptic weather stations world-wide, see [6] and [20]. This removes systematic biases and provides calibrated (statistically unbiased) point probabilities.

We describe the available data, which has been computed according to the method stated above. Our application covers a time frame of four months in the year 2012 including a summer period from June 1 until July 31 and a winter period from November 1 until December 31 in order to consider different seasons. For each day of the time frame seven one-hour forecast periods from 02-03 UTC (Universal Time, Coordinated) every three hours up to 20-21 UTC are available. Furthermore, we consider a system of 503 weather stations, which are located inside the territories of Germany and Luxembourg. For each forecast period and each weather station, a sequence of point probabilities for the occurrence of precipitation of more than u mm is available for thresholds $u \in T = \{0, 0.1, 0.2, 0.3, 0.5, 0.7, 1, 2, 3, 5, 10, 15\}$. In particular, for $u = 0$ the probability for precipitation of any amount at the considered weather station is given. We use the data later on for implementation and verification of the presented modeling approach.

3 Stochastic model for the occurrence of precipitation

We briefly recall a stochastic model for the occurrence of precipitation, which has been introduced in [8]. This provides a basis for the modeling of precipitation amounts as described in Sect. 4. In the following, a fixed forecast period and a probability space $(\Omega, \mathcal{F}, P)$ are considered, where Ω is a set containing all possible precipitation scenarios and the corresponding predictions of the numerical weather forecast models of DWD, $\mathcal{F}$ is a σ-algebra of subsets of Ω (so-called events) and P is a suitable probability measure, which associates each event $A \in \mathcal{F}$ with the probability $P(A) \in [0, 1]$ of its occurrence. We describe the model in a general context. Let $s_1, \ldots, s_n$ be a sequence of geographically distinct points (e.g., the sites of weather stations), which are located within a bounded and convex sampling window $W \subset \mathbb{R}^2$. The true characteristics describing future weather conditions, as e.g. point probabilities for the occurrence of precipitation or expected precipitation amounts at $s_1, \ldots, s_n$, are typically unknown and cannot be determined exactly. However, most of these characteristics can be estimated using numerical models and statistical post-processing, see e.g. Sect. 2. By applying the MOS approach, systematic errors in estimated point probabilities are eliminated but the

[1] The GME has been substituted in January 2015 by the Icosahedral Non-hydrostatic (ICON) General Circulation Model, see [24].

estimators are still subject to random errors. To account for that, we introduce the random variable $E : \Omega \to \mathbb{S}$ describing the random error of the weather forecast models used by DWD, where $\mathbb{S}$ is the space of all possible errors. Since estimators of point probabilities depend on the random error E, they are also considered to be random variables in the following (as usually done in estimation theory). For that purpose, we introduce the random field $\{P_t, t \in W\}$, where $P_t : \Omega \to [0,1]$ represents the random point probability for the occurrence of precipitation at location $t \in W$. For any fixed $t \in W$, the random variable P_t is assumed to be $\sigma(E)$-measurable, where $\sigma(E) \subset \mathcal{F}$ is the sub-σ-algebra of events generated by E. This implies that if conditioned on $\{E = e\}$ for any realization e of E, the value of P_t is non-random (and only depends on e). This value is identified by the conditional expectation $\mathbb{E}(P_t \mid E = e)$. Heuristically, conditioning on $\{E = e\}$ for $e \in \mathbb{S}$ means that a concrete realization of the weather forecast models of DWD (with error e) is given (which is always the case in applications). We suppose that the available data include a sequence $p^{(0)}_{s_1} = \mathbb{E}(P_{s_1} \mid E = e), \ldots, p^{(0)}_{s_n} = \mathbb{E}(P_{s_n} \mid E = e)$ of point probabilities, which are computed based on a particular realization e of E. In our example of application we consider the available point probabilities for the occurrence of precipitation described in Sect. 2, $n = 503$ is the number of considered weather stations and e is the error that occurs when providing these data.

The fundamental assumption of our modeling approach is that there is precipitation at any location $t \in W$ if and only if t is covered by at least one precipitation cell. To allow for spatially varying precipitation probabilities we furthermore suppose that precipitation cells (i.e., their cell centers) occur according to a random location-dependent intensity function $\{\Lambda_t, t \in W\}$ with $\Lambda_t : \Omega \to [0,\infty)$ being the random intensity for the formation of precipitation cells at $t \in W$. Again, the value of Λ_t is non-random conditioned on $\{E = e\}$ for any $e \in \mathbb{S}$, i.e., Λ_t is assumed to be $\sigma(E)$-measurable, for all $t \in W$. To account for the fact that data are only available at the sites $s_1, \ldots, s_n$ we make the simplifying assumption that realizations of $\{\Lambda_t, t \in W\}$ are piecewise constant in a neighborhood of each site s_i for $i = 1, \ldots, n$. The most natural choice of such a neighborhood is the Voronoi tessellation $\{V(s_1), \ldots, V(s_n)\}$ of $s_1, \ldots, s_n$ in W, where the Voronoi cell $V(s_i)$ of s_i is defined as

$$V(s_i) = \{x \in W : |x - s_i| < |x - s_j| \text{ for all } j = 1, \ldots, n \text{ with } j \neq i\} \tag{1}$$

for $i = 1, \ldots, n$ and $|x - s|$ denotes the Euclidean distance between $x \in W$ and $s \in W$. Accordingly, $\{\Lambda_t, t \in W\}$ is represented as

$$\Lambda_t = \sum_{j=1}^{n} A_j \, I_{V(s_j)}(t) \quad \text{for all } t \in \bigcup_{i=1}^{n} V(s_i), \tag{2}$$

where the $\sigma(E)$-measurable random variables $A_1, \ldots, A_n : \Omega \to [0,\infty)$ can be interpreted as random local intensities for the formation of precipitation cells in neighborhoods of $s_1, \ldots, s_n$. The function $I_V : W \to \{0,1\}$ denotes the indicator of the set $V \subset W$. If $t \in W$ is not located within any of the Voronoi cells, i.e., it is located on the boundaries of one or more cells, then Λ_t is set equal to the minimum intensity of all adjacent Voronoi cells. For the modeling of centers of precipitation cells a two-dimensional Cox point process $\{X_i, i = 1, \ldots, Z\}$ in W

with intensity function $\{\Lambda_t, t \in W\}$ is used, see e.g. [1], where the random variable $Z : \Omega \to \{0, 1, \ldots\}$ describes the total number of precipitation cells in W.

Due to the irregularity of precipitation patterns it seems hardly possible to give a model for the shape of precipitation cells, which exactly represents typical precipitation patterns and, simultaneously, is still easy to handle. We rather assume that there is precipitation at location $t \in W$ if t is close enough to the center of at least one precipitation cell. This is equivalent to saying that t is covered by the germ-grain model

$$M = \bigcup_{i=1}^{Z} b(X_i, R), \tag{3}$$

where $b(x, r) = \{y \in \mathbb{R}^2 : |y - x| \leq r\}$ denotes the two-dimensional ball with center $x \in \mathbb{R}^2$ and radius $r > 0$ and the random variable $R : \Omega \to (0, \infty)$ can be interpreted as spatial precipitation range. We assume that R is $\sigma(E)$-measurable, i.e., R is non-random conditioned on $\{E = e\}$ for any $e \in \mathbb{S}$. Although it is obvious that precipitation cells are typically not circular in real precipitation patterns, they are often approximated as circular or elliptical discs in the literature, see e.g. [15], [16] and [19]. Thus, we will also interpret the germ-grain model M as an approximate representation for the union set of precipitation cells in the following. Note that conditioned on $\{E = e\}$ for any realization e of E, the Cox process $\{X_i, i = 1, \ldots, Z\}$ is a Poisson process with (deterministic) intensity function $\{\lambda_t, t \in W\}$, where $\lambda_t = \mathbb{E}(\Lambda_t \,|\, E = e)$ for $t \in W$, and M is a Boolean model based on $\{X_i, i = 1, \ldots, Z\}$ with grain radius $r = \mathbb{E}(R \,|\, E = e)$, see e.g. [1] or [4]. In application, where a particular realization of the weather forecast models of DWD providing the underlying data is given (and thus a realization e of E is considered) we assume the distribution of future precipitation fields, described by $\{\lambda_t, t \in W\}$ and r, to be deterministic. Both $\{X_i, i = 1, \ldots, Z\}$ and M, however, which represent the still unknown future precipitation scenario, are still considered to be random (i.e., not $\sigma(E)$-measurable). Finally, point probabilities are modeled as (conditional) coverage probabilities of the union set M of precipitation cells, i.e., the random point probability P_t is represented as $P_t = P(t \in M \,|\, E)$ for $t \in W$. We will show in Sect. 5 how these settings are used to compute point and area probabilities for the occurrence of precipitation as (conditional) coverage probabilities of the germ-grain model M in applications. In order to do this, the intensity function $\{\lambda_t, t \in W\}$ and the precipitation range r (given $e \in \mathbb{S}$) need to be represented in terms of the available data. Since this is of minor importance for the main objective of the present paper, the modeling of precipitation amounts, we refer to [8] for further details.

4 Stochastic model for precipitation amounts

4.1 Model description

The computation of area probabilities for precipitation exceeding various thresholds based solely on a model for precipitation cells does not seem to be possible. Therefore, the additional modeling of precipitation amounts is required. For that purpose, we introduce the random field $\{\Gamma_t, t \in W\}$, where $\Gamma_t : \Omega \to [0, \infty)$ is interpreted as the random amount of precipitation at location $t \in W$. We expect that precipitation cells and precipitation amounts cannot be considered to be independent of one another, which is also indicated by the results of a statistical test performed in [7]. Thus, we suggest to represent $\{\Gamma_t, t \in W\}$ as a random shot-noise field. Note that this class of random fields has already been used in the literature for the modeling of precipitation amounts, see e.g. [16]. At first, a symmetric response function $K_p(\cdot, X_i, R)$ is assigned to each precipitation cell $b(X_i, R)$ for $i = 1, \dots, Z$, where we choose $K_p : \mathbb{R}^2 \times \mathbb{R}^2 \times (0, \infty) \to [0, \infty)$ with

$$K_p(t, x, r) = \left(1 - \frac{|t - x|^2}{r^2}\right)^p I_{b(t,r)}(x) \quad \text{for all } t, x \in \mathbb{R}^2, r > 0. \tag{4}$$

Here, $p > 0$ is a certain shape parameter. This choice comprises a variety of possible response functions, e.g., the upper half of the unit ball ($p = 0.5$), a scaled version of the Epanechnikov kernel ($p = 1$), a scaled version of the biweight kernel ($p = 2$) or a scaled version of the triweight kernel ($p = 3$). However, these response functions are not yet suitable to model precipitation fields generated by single precipitation cells since the distribution of precipitation amounts should vary spatially for most forecast periods. An example would be the forecast shown in Fig. 2, where clearly higher precipitation amounts are expected in the north and west than in the south and east part of the sampling window. For that purpose, each response function $K_p(\cdot, X_i, R)$ is multiplied by a random location-dependent scaling variable. We suppose that information on expectation and variance of point precipitation amounts is only available at $s_1, \dots, s_n$, so we make the simplifying assumption that all precipitation cells with centers in a given Voronoi cell $V(s_i)$ are multiplied by the same scaling variable for $i = 1, \dots, n$. Thus, we consider a sequence $C_1, \dots, C_n : \Omega \to [0, \infty)$ of non-negative random scaling variables, which correspond to the n Voronoi cells $V(s_1), \dots, V(s_n)$. Again, $C_1, \dots, C_n$ can clearly not be assumed to be $\sigma(E)$-measurable since they are still random for a given realization of the weather forecast models of DWD. However, we assume that conditioned on E, the variables $C_1, \dots, C_n$ are independent of each other and of the point process $\{X_i, i = 1, \dots, Z\}$ of precipitation cell centers. For each $t \in W$, we interpret the value of the response function $K_p(t, X_i, R)$ multiplied by the corresponding scaling variable as the random amount of precipitation generated by the i-th precipitation cell $b(X_i, R)$ at location t. The total amount of precipitation at $t \in W$ is obtained by summing up the individual precipitation amounts generated by all Z precipitation cells. Combining the modeling steps suggested above leads to the following representation formula for the random amount of precipitation Γ_t at location t:

$$\Gamma_t = \sum_{i=1}^{Z} \sum_{j=1}^{n} C_j I_{V(s_j)}(X_i) K_p(t, X_i, R) \quad \text{for all } t \in W. \tag{5}$$

The consecutive steps of this modeling approach are illustrated in Fig. 1.

The random field $\{\Gamma_t, t \in W\}$ of precipitation amounts is completely described by the Cox process $\{X_i, i = 1, \dots, Z\}$ of cell centers (which in turn is characterized by the local random intensities $\Lambda_1, \dots, \Lambda_n$), the random precipitation range R, the local random scaling variables $C_1, \dots, C_n$ and the shape parameter p. In the following, let e be a particular realization of the random error E that occurs

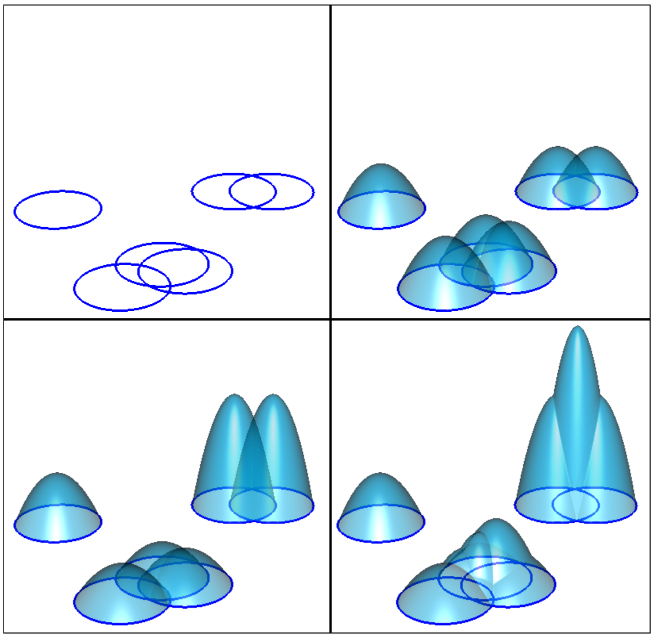

Fig. 1 Illustration of the modeling approach for precipitation amounts: (i) modeling of precipitation cells using a germ-grain model with circular grains (top left), (ii) assigning a symmetric response function to each cell (top right), (iii) multiplying response functions with random scaling variables (bottom left), (iv) summing scaled response functions to obtain precipitation amounts (bottom right).

when computing the underlying data using the weather forecast models of DWD. Recall that the (conditional) intensities $a_1 = \mathbb{E}(A_1 \mid E = e), \ldots, a_n = \mathbb{E}(A_n \mid E = e)$ and the precipitation range $r = \mathbb{E}(R \mid E = e)$ are computed based on the corresponding point probabilities $p^{(0)}_{s_1} = \mathbb{E}(P_{s_1} \mid E = e), \ldots, p^{(0)}_{s_n} = \mathbb{E}(P_{s_n} \mid E = e)$, see Sect. 3 or [8]. It remains to fit (conditional) distributions of the random scaling variables $C_1, \ldots, C_n$ and to choose a suitable shape parameter p. For that purpose we introduce the deterministic fields $\{\mu_t, t \in W\}$ and $\{v_t, t \in W\}$, where $\mu_t = \mathbb{E}(\mathit{\Gamma}_t \mid E = e) \in [0, \infty)$ denotes the conditional expectation of $\mathit{\Gamma}_t$ and $v_t = \mathrm{var}(\mathit{\Gamma}_t \mid E = e) \in [0, \infty)$ the conditional variance of $\mathit{\Gamma}_t$ given $\{E = e\}$ for all $t \in W$.

4.2 Fitting the distributions of precipitation amounts at weather stations

In Sect. 4.3 below, we suggest a procedure to fit the distributions of the random scaling variables $C_1, \ldots, C_n$ based on data given for the locations of weather stations. Recall that for each station $s \in \{s_1, \ldots, s_n\}$ the available data described in Sect. 2 include a sequence of point probabilities for the occurrence of precipitation of more than u mm for thresholds $u \in T = \{0, 0.1, 0.2, 0.3, 0.5, 0.7, 1, 2, 3, 5, 10, 15\}$. Furthermore, using the probability for the occurrence of precipitation, the (conditional) probability of precipitation exceeding u mm (given that precipitation occurs) can be computed for all thresholds $u \in T \setminus \{0\}$. However, these data are not yet suitable for model fitting. On the one hand, point probabilities are expected to be monotonically decreasing with increasing threshold $u \in T$ in mm.

By using the MOS approach in the post-processing step, however, the probabilities of each threshold are computed separately, which does not guarantee monotonicity due to statistically independent noise. In a few cases in our data it is possible that, e.g., the probability of precipitation of more than 0.3 mm at a given weather station is slightly higher than the probability of precipitation of more than 0.2 mm. On the other hand, expectations and variances of point precipitation amounts, which are needed for model fitting, are not directly included in the data. To overcome both problems we assume that if precipitation occurs, then the random precipitation amounts at the weather stations $s_1, \ldots, s_n$ are gamma distributed as suggested e.g. in [20] and [21]. For a fixed weather station $s \in \{s_1, \ldots, s_n\}$ and a particular realization e of E, consider the (conditional) probabilities $p_s^{(u)} = P(\Gamma_s > u \mid E = e)$ for all $u \in T$, where Γ_s denotes the random precipitation amount at location $s \in W$ as introduced at the beginning of Sect. 4.1. However, the gamma distribution is not directly suitable for the modeling of Γ_s (given $E = e$) since the gamma distribution is an absolutely continuous distribution and $P(\Gamma_s = 0 \mid E = e) > 0$ in general. Thus, as described before, only positive precipitation amounts are modeled using the gamma distribution. For that purpose, we consider the conditional probabilities $\tilde{p}_s^{(u)} = P(\Gamma_s > u \mid \Gamma_s > 0, E = e)$ for the occurrence of precipitation of more than u mm given that precipitation of any (positive) amount occurs at s for each threshold $u \in T \setminus \{0\}$. Then, the parameters of a gamma distribution are fitted based on the (conditional) probabilities of precipitation exceeding u mm, $u \in T \setminus \{0\}$, given that precipitation occurs at weather station s, which were derived from the data before. This allows to analytically compute the sequence $\{\tilde{p}_s^{(u)}, u \in T \setminus \{0\}\}$ of (conditional) probabilities based on the fitted gamma distribution. We also compute the conditional expectations $\tilde{\mu}_s = \mathbb{E}(\Gamma_s \mid \Gamma_s > 0, E = e)$ and $\tilde{m}_s = \mathbb{E}(\Gamma_s^2 \mid \Gamma_s > 0, E = e)$ according to the fitted gamma distribution. Finally, the point probabilities $p_s^{(u)}$ for $u \in T \setminus \{0\}$ can be recomputed easily using the identity $p_s^{(u)} = p_s^{(0)} \tilde{p}_s^{(u)}$, where the zero-level probability $p_s^{(0)}$ is directly taken from the data. This approach has the advantage that the point probabilities $\{p_s^{(u)}, u \in T\}$ are now monotonically decreasing with increasing threshold u. Moreover, the fitted gamma distribution allows to easily compute the expectation μ_s and variance v_s of Γ_s (conditioned on $\{E = e\}$) according to $\mu_s = \mathbb{E}(\Gamma_s \mid E = e) = p_s^{(0)} \tilde{\mu}_s$ and $v_s = \mathrm{var}(\Gamma_s \mid E = e) = p_s^{(0)} \tilde{m}_s - \mu_s^2$. Fig. 2 illustrates some sample data for a given forecast period. Note that precipitation of more than 5, 10 or 15 mm is considered to be an extreme event since the corresponding point probabilities are close to zero in almost all cases.

4.3 Fitting the distributions of random scaling variables

In this section, we introduce an approach to fitting (conditional) distributions of the random scaling variables $C_1, \ldots, C_n$. At first, we state formulas for the conditional expectation μ_t and variance v_t of Γ_t conditioned on $\{E = e\}$. It holds that:

$$\mu_t = \sum_{j=1}^{n} \mathbb{E}(C_j \mid E = e)\, a_j I(s_j, t) \tag{6}$$

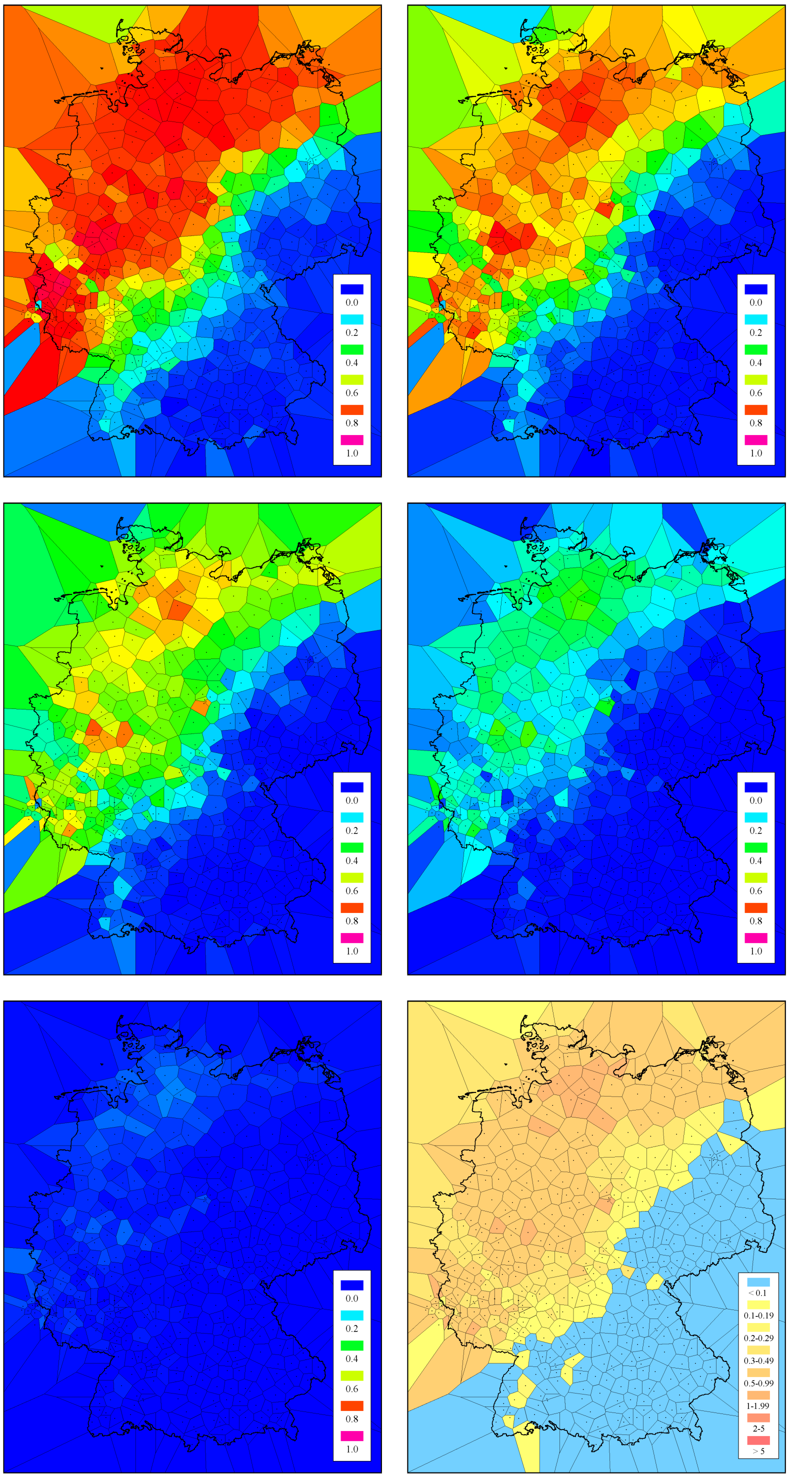

Fig. 2 Sample data for December 25, 2012, 11-12 UTC obtained from the fitted gamma distribution: the locations of the considered 503 weather stations and the corresponding Voronoi tessellation, see equation (1), where each Voronoi cell is colored according to the point probability for the occurrence of precipitation of more than 0 mm (top left), 0.1 mm (top right), 0.3 mm (center left), 1 mm (center right) and 3 mm (bottom left) or the expected precipitation amount (bottom right).

and

$$v_t = \sum_{j=1}^{n} \mathrm{var}(C_j \mid E = e) \left[a_j \tilde{I}(s_j, t) + a_j^2 I^2(s_j, t) \right] + \sum_{j=1}^{n} (\mathbb{E}(C_j \mid E = e))^2 a_j \tilde{I}(s_j, t) \tag{7}$$

for all $t \in W$, where

$$I(s_j, t) = \int_{V(s_j) \cap b(t,r)} \left(1 - \frac{|t-x|^2}{r^2}\right)^p \mathrm{d}x \tag{8}$$

and

$$\tilde{I}(s_j, t) = \int_{V(s_j) \cap b(t,r)} \left(1 - \frac{|t-x|^2}{r^2}\right)^{2p} \mathrm{d}x. \tag{9}$$

A derivation of equations (6) and (7) is given in the appendix. We suppose that the expectations $\mu_{s_1} = \mathbb{E}(\Gamma_{s_1} \mid E = e), \ldots, \mu_{s_n} = \mathbb{E}(\Gamma_{s_n} \mid E = e)$ and variances $v_{s_1} = \mathrm{var}(\Gamma_{s_1} \mid E = e), \ldots, v_{s_n} = \mathrm{var}(\Gamma_{s_n} \mid E = e)$ of point precipitation amounts at $s_1, \ldots, s_n$ can be computed from available data. In our example of application, $\mu_{s_1}, \ldots, \mu_{s_{503}}$ and $v_{s_1}, \ldots, v_{s_{503}}$ are the expectations and variances that were obtained from the fitted gamma distributions in Sect. 4.2 and e is the particular error of the weather forecast models of DWD when computing the underlying data. By $c_j = \mathbb{E}(C_j \mid E = e)$ and $\tilde{c}_j = \mathrm{var}(C_j \mid E = e)$ we denote the conditional expectation and variance of C_j given $\{E = e\}$ for $j = 1, \ldots, n$. Intuitively, $c_1, \ldots, c_n$ should be chosen in such a way that (6) holds for $t = s_1, \ldots, s_n$. This results in a system of n linear equations with unknown variables $c_1, \ldots, c_n$. In general, this system of equations cannot be solved exactly under the constraint that $c_1, \ldots, c_n \geq 0$. Thus, we compute $c_1, \ldots, c_n$ in a nonnegative least-squares sense, i.e.,

$$(c_1, \ldots, c_n) = \underset{c'_1, \ldots, c'_n \geq 0}{\operatorname{argmin}} \left\{ \sum_{i=1}^{n} \left(\mu_{s_i} - \sum_{j=1}^{n} c'_j \, a_j I(s_j, s_i) \right)^2 \right\}, \tag{10}$$

see [12]. Analogously, $\tilde{c}_1, \ldots, \tilde{c}_n$ should satisfy (7) for $t = s_1, \ldots, s_n$. Again, this results in a system of n linear equations with unknown variables $\tilde{c}_1, \ldots, \tilde{c}_n$. Due to the constraint $\tilde{c}_1, \ldots, \tilde{c}_n \geq 0$ we solve the system of equations in a nonnegative least-squares sense, too, i.e.,

$$\begin{aligned}(\tilde{c}_1, \ldots, \tilde{c}_n) = \underset{c'_1, \ldots, c'_n \geq 0}{\operatorname{argmin}} \Bigg\{ \sum_{i=1}^{n} \Bigg(v_{s_i} &- \sum_{j=1}^{n} c_j^2 a_j \tilde{I}(s_j, s_i) \\ &- \sum_{j=1}^{n} c'_j \left[a_j \tilde{I}(s_j, s_i) + a_j^2 I^2(s_j, s_i) \right] \Bigg)^2 \Bigg\}.\end{aligned} \tag{11}$$

Now, knowing the (conditional) expectations and variances of the local scaling variables $C_1, \ldots, C_n$, we fit a two-parameter distribution to each C_i using the method of moments. We suggest to use one of the following parametric families of distributions: beta prime, gamma, inverse gamma, inverse normal or log-normal. These distributions seem to be the most suitable ones since they are defined on the nonnegative real line, have finite second moments[2] and their parameters can be represented as closed functions of expectation and variance, which is required for applying the method of moments. Finally, all (conditional) characteristics of the random field $\{\Gamma_t, t \in W\}$ given $\{E = e\}$ have been determined: the local intensities $a_1, \ldots, a_n$ for the formation of precipitation cells, the precipitation range r and the (conditional) distributions of the local scaling variables $C_1, \ldots, C_n$. Note that the type of distributions of local scaling variables as well as the shape parameter p of the response function K_p are chosen globally (i.e., for all forecast periods). A recommendation on how to make this model choice in practice is given in Sect. 6.

5 Model-based estimation of area probabilities

The combined model for precipitation cells and precipitation amounts introduced in Sect. 3 and 4 allows for the computation of point and area probabilities for the occurrence of precipitation exceeding an arbitrary threshold $u \geq 0$. Again, we consider a particular realization e of the random error E and the corresponding model characteristics $a_1, \ldots, a_n$ and r. A central assumption of our modeling approach is that there is precipitation at any location $t \in W$ if and only if t is covered by the germ-grain model M of precipitation cells introduced in equation (3). Accordingly, the point probability $p_t^{(0)}$ for the occurrence of precipitation at any location $t \in W$ is given by $p_t^{(0)} = P(t \in M \,|\, E = e)$. Note that the following closed formula for $p_t^{(0)}$ holds, see [8]:

$$p_t^{(0)} = 1 - \exp\left(-\sum_{j=1}^{n} a_j\, \nu_2\left(b(t,r) \cap V(s_j)\right)\right) \quad \text{for all } t \in W, \tag{12}$$

where ν_2 denotes the two-dimensional Lebesgue measure. Analogously, we assume that there is precipitation somewhere within an area $B \subset W$ if B intersects M. Thus, the area probability $\pi^{(0)}(B)$ for the occurrence of precipitation in any Borel set $B \subset W$ is given by $\pi^{(0)}(B) = P(B \cap M \neq \emptyset \,|\, E = e)$, where the following representation formula holds, see [8]:

$$\pi^{(0)}(B) = 1 - \exp\left(-\sum_{j=1}^{n} a_j\, \nu_2\left((B \oplus b(o,r)) \cap V(s_j)\right)\right). \tag{13}$$

Here, $o \in \mathbb{R}^2$ denotes the origin and $A \oplus B = \{x + y, x \in A, y \in B\}$ is the Minkowski sum of two sets $A, B \subset W$.

The above approach can be generalized as follows. We suppose that for any threshold $u \geq 0$, there is precipitation of more than u mm at $t \in W$ if $\Gamma_t > u$. This implies that the point probability $p_t^{(u)}$ for more than u mm of precipitation at any location $t \in W$ is given by $p_t^{(u)} = P(\Gamma_t > u \,|\, E = e)$, see Sect. 4.2. Similarly, we suppose that there is precipitation of more than u mm somewhere within an area $B \subset W$ if $\Gamma_t > u$ for some $t \in B$. Thus, the area probability

[2] For beta prime and inverse gamma distribution only those parameter configurations are considered that lead to a finite variance.

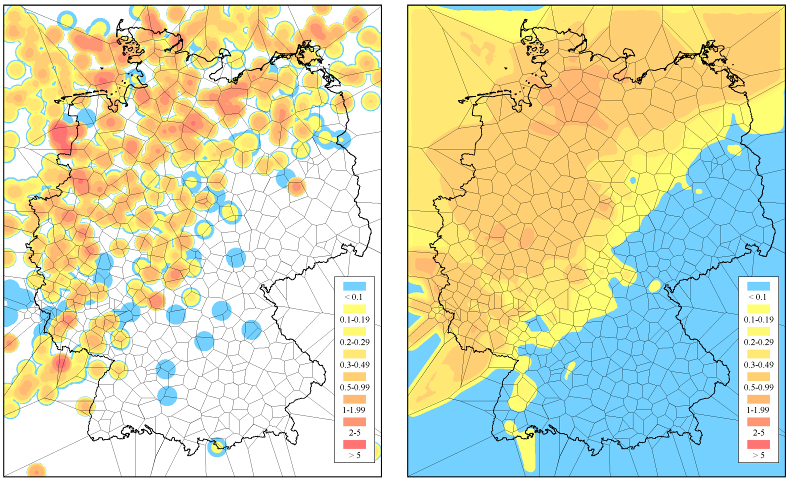

Fig. 3 Simulation results for December 25, 2012, 11-12 UTC: typical realization of the random field $\{\Gamma_t, t \in W\}$ of precipitation amounts given in equation (5) (left) and mean precipitation amounts estimated based on 5000 realizations of $\{\Gamma_t, t \in W\}$ (right).

$\pi^{(u)}(B)$ for the occurrence of precipitation exceeding u somewhere in B is given by $\pi^{(u)}(B) = P(\max\{\Gamma_t, t \in B\} > u \,|\, E = e)$. Unfortunately, for both these point and area probabilities no closed representation formulas are known. As an alternative we suggest to estimate $p_t^{(u)}$ and $\pi^{(u)}(B)$ by repeated simulation of the fitted random field $\{\Gamma_t, t \in W\}$ of precipitation amounts given $\{E = e\}$. In order to do so, we generate a large number of realizations of the germ-grain model M and of the random scaling variables $C_1, \ldots, C_n$ and estimate the desired probabilities as relative frequencies of the considered events among all realizations. In Fig. 3 simulation results for a forecast period selected from our example of application are illustrated. A comparison with Fig. 2 shows that the results agree well with the underlying data.

6 Implementation and forecast verification

The combined model for precipitation cells and precipitation amounts has been implemented in Java using the GeoStoch library, see [14]. We compute the model characteristics for all forecast periods described in Sect. 2 using the available point probabilities at the locations $s_1, \ldots, s_n$ of the $n = 503$ weather stations and the expectations and variances of point precipitation amounts obtained from the fitted gamma distributions as described in Sect. 4.2.

6.1 Choice of model configuration

At first, a comparison between the point probabilities estimated according to the proposed model and those obtained from the fitted gamma distributions is made in order to give a recommendation on how to choose the shape parameter p and the type of (conditional) distributions of the local scaling variables. We consider p to take one of the five values from $\{0.5, 1, 2, 3, 4\}$ and the following types of two-parameter distributions for the scaling variables: beta prime, gamma, inverse gamma, inverse normal and log-normal. Choosing $p > 4$ does not lead to significant changes in estimated probabilities compared to $p = 4$. For each value of p, each distribution type and each threshold $u \in \{0.1, 0.2, 0.3, 0.5, 0.7, 1, 2, 3, 5, 10, 15\}$, point probabilities at $s_1, \ldots, s_{503}$ are estimated for all available forecast periods as described in Sect. 5. Then, a comparison with the point probabilities obtained from the fitted gamma distributions, see Sect. 4.2, is made. For each shape parameter, distribution type, threshold and weather station, the bias, correlation coefficient and mean squared difference (msd) are computed using the point probabilities of all forecast periods. Since this results in a huge amount of computed values, the scores are averaged once more over all weather stations. Note that near the boundaries of the sampling window no consistent estimation of (point and area) probabilities can be guaranteed due to edge effects and thus, only weather stations inside the boundaries of Germany are taken into account here. The results yield that for all thresholds and shape parameters, the correlation coefficients and msd's perform best when using gamma distributions for the local scaling variables. However, the effect of changing this type of distribution seems to be minor since only small variations in the scores are observed. Similar results are found when analyzing the effect of changing the shape parameter. The scaled Epanechnikov kernel ($p = 1$) leads to the smallest msd's and highest correlation coefficients but only minor differences are observed for $p = 2, 3, 4$ (see also Table 1 in [9]). Only the upper half of the unit ball ($p = 0.5$) produces larger biases and msd's making it inappropriate for the use as response function. Since the computed scores vary only slightly for most shape parameters and distribution types, we also consider a verification of area probabilities using radar data in order to give a final recommendation on how to choose these model configurations, see Sect. 6.2.

6.2 Verification of area probabilities using radar data

We compare estimated area probabilities with precipitation indicators derived from independent rain gauge adjusted radar data. As test areas we choose the Voronoi cells $V(s_1), \ldots, V(s_{503})$ that correspond to the locations $s_1, \ldots, s_{503}$ of the 503 weather stations. The Voronoi cells are suitable for verification since they include areas of different shape, size and orientation. Again, for each value of p and each distribution type as described in Sect. 6.1, area probabilities for $V(s_1), \ldots, V(s_{503})$ are estimated according to the procedure explained in Sect. 5 for all available forecast periods and thresholds $u \in \{0.1, 0.2, 0.3, 0.5, 0.7, 1, 2, 3, 5, 10, 15\}$. Hourly accumulated precipitation amounts for all considered forecast periods are obtained from the German operational radar network of DWD, see [22]. To each estimated area probability for the occurrence of precipitation of more than u mm somewhere in a Voronoi cell $V(s_i)$, $i = 1, \ldots, n$, we assign the corresponding precipitation indicator, which is 1 if there is precipitation of more than u mm somewhere within $V(s_i)$ with respect to radar data and 0 otherwise.

The following three scores are considered in order to compare area probabilities and precipitation indicators for fixed thresholds. For each threshold and each Voronoi cell, the bias, the Brier skill score and the empirical correlation coefficient are computed based on estimated area probabilities and precipitation indicators for all forecast periods. Again, only Voronoi cells inside the boundaries of Germany are taken into account to avoid edge effects. The bias is simply the difference of the mean probability and the mean precipitation indicator and the correlation coefficient should be self-explanatory. The Brier skill score, however, is more difficult to explain, see also Chap. 8 in [20]. At first, the Brier score BS is determined as the mean squared difference of estimated area probabilities and precipitation indicators. This score, however, is difficult to interpret and thus, the Brier score $\widetilde{BS}$ of a reference forecast is additionally determined. As reference method we use the climate mean, where each probability is given as the mean precipitation indicator. The Brier skill score is then defined as $1 - BS/\widetilde{BS}$. Of course, area probabilities computed from our precipitation model should be more precise than the climate mean, which is why the Brier skill score is required to be clearly positive. To increase the significance of the verification results, all three scores are only computed if the corresponding weather event occurs at least 10 times in the considered time period.

At first, we analyze the performance of the three scores when varying the shape parameter p and the type of the (conditional) distributions of the local scaling variables $C_1, \ldots, C_{503}$. The results confirm what we found in Sect. 6.1. For almost all shape parameters and thresholds, the gamma distribution yields the highest Brier skill scores and correlation coefficients, although the choice of the type of the scaling distributions has a minor effect. A more noticeable impact (particularly on the bias) is observed when changing the value of the shape parameter p. It seems that larger values of p are more appropriate when computing area probabilities for higher thresholds. To obtain a bias that is as close as possible to 0 we recommend to use the scaled Epanechnikov kernel ($p = 1$) for thresholds smaller than 0.2 mm, the scaled biweight kernel ($p = 2$) for thresholds between 0.2 and 0.5 mm and the scaled triweight kernel ($p = 3$) for thresholds of at least 0.5 mm. A larger p can improve the bias even more for thresholds of more than 1 mm but this will also lead to decreasing Brier skill scores and correlation coefficients and is therefore not recommended.

We analyze the bias, Brier skill score and correlation coefficient of estimated area probabilities and precipitation indicators, where the model configuration suggested above is used. Since estimated area probabilities are expected to depend heavily on the precision of the underlying input data, we also provide a comparison of point probabilities for the locations of the weather stations obtained according to the fitted gamma distributions (which in turn are based on the point probabilities provided by DWD) and precipitation indicators derived from radar data. Again, the bias, the Brier skill score and the empirical correlation coefficient are taken into account, where scores are only computed for those weather stations at which the corresponding weather event occurs at least 10 times during the considered time period. This implies, however, that no verification of point probabilities for thresholds of 5 mm or higher is possible. To avoid edge effects, only weather stations and Voronoi cells inside the boundaries of Germany are considered. Scores for each threshold are visualized using boxplots in Fig. 4 for point probabilities and in Fig. 5 for area probabilities.

When analyzing mean biases for estimated area probabilities, we find that there is no systematic error for all thresholds up to 5 mm, whereas area probabilities seem to be slightly too low for thresholds of 10 and 15 mm. More variation is observed for single Voronoi cells. Although the bias is close to zero for most areas,

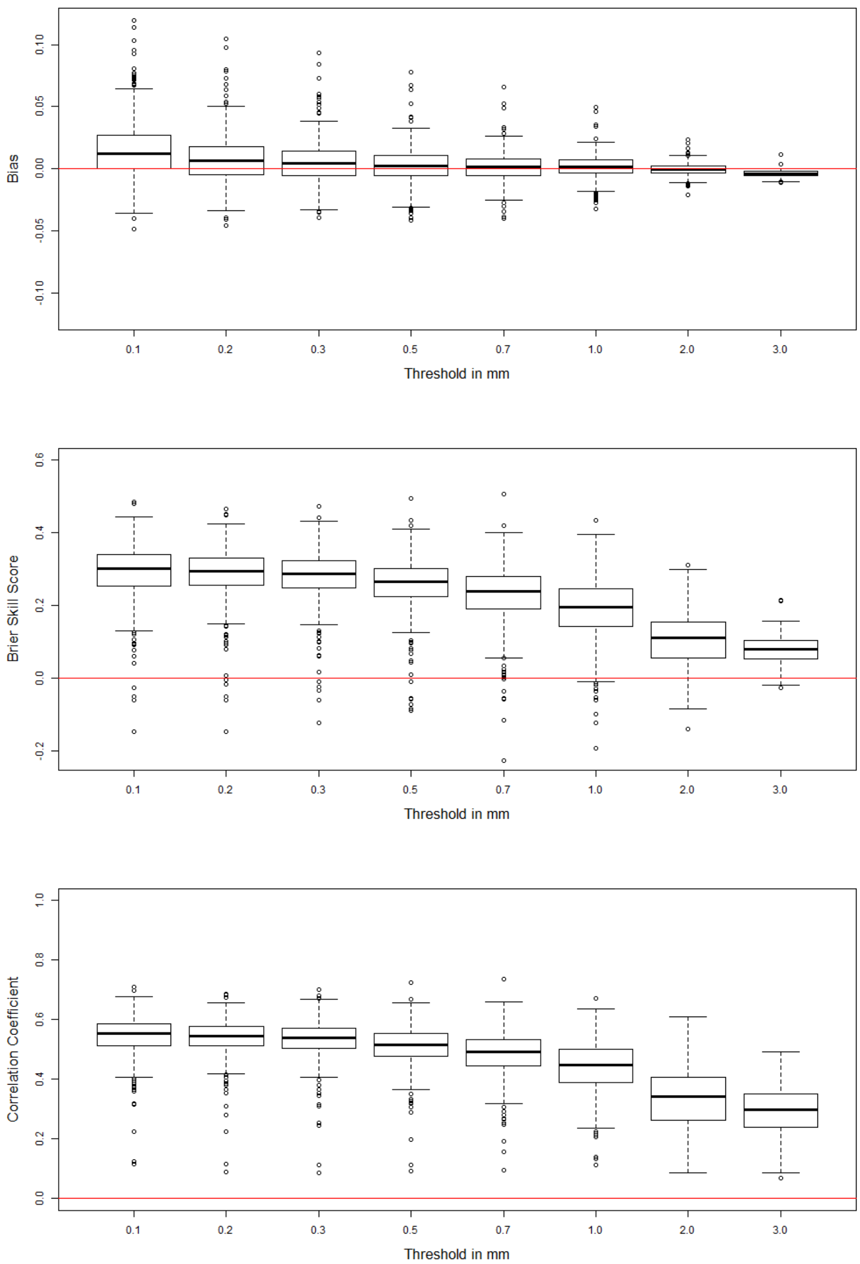

Fig. 4 Forecast verification using radar data: scores of point probabilities that are obtained by fitting gamma distributions to data provided by DWD. For a sequence of thresholds the biases (top), Brier skill scores (center) and correlation coefficients (bottom) of all stations inside the boundaries of Germany are visualized as boxplots. Thresholds of 5 mm and more are not considered since the corresponding weather events occur less than 10 times at all weather stations.

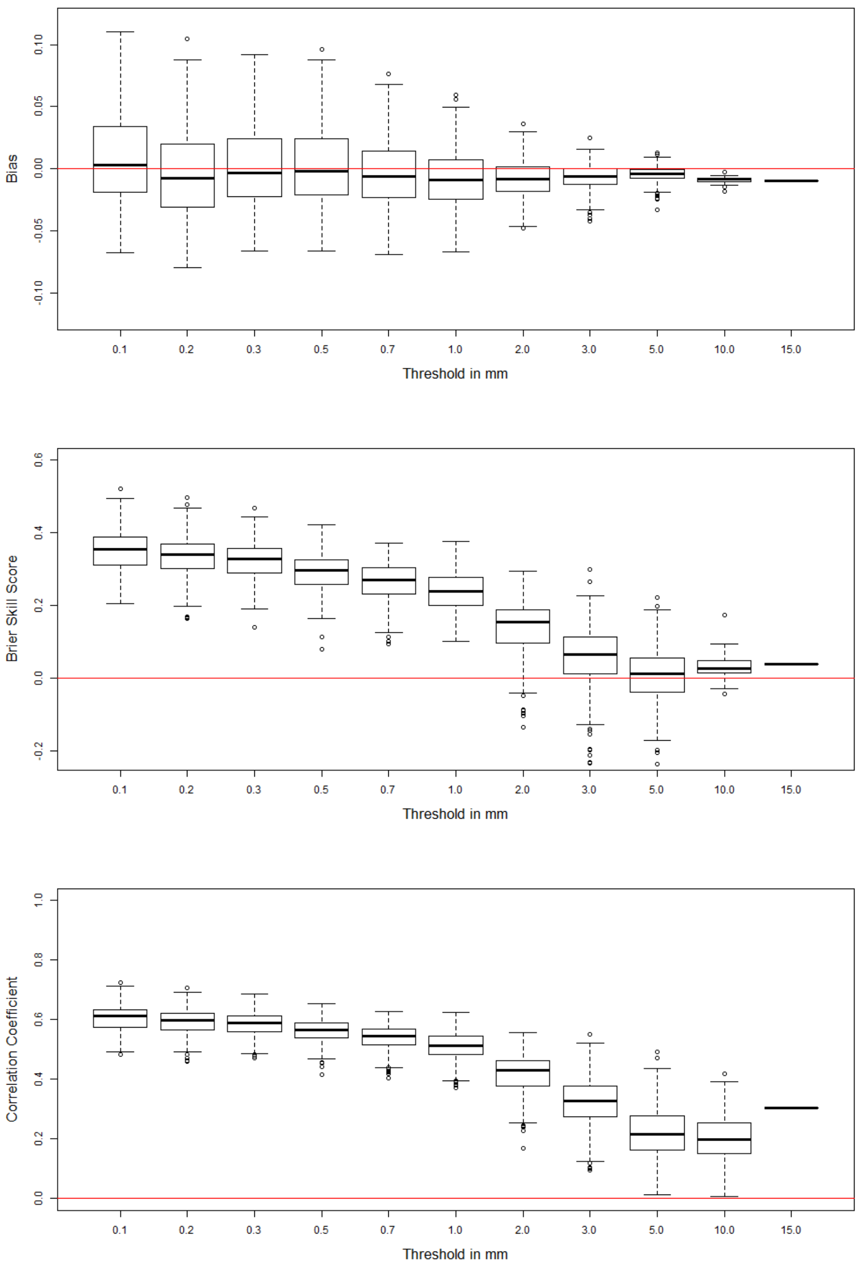

Fig. 5 Forecast verification using radar data: scores of area probabilities that are estimated based on the proposed precipitation model. For a sequence of thresholds the biases (top), Brier skill scores (center) and correlation coefficients (bottom) of all Voronoi cells inside the boundaries of Germany are visualized as boxplots. For thresholds of 5 mm and more only those Voronoi cells are considered where the corresponding weather event occurs at least 10 times.

we occasionally obtain values reaching up to -6% or $+10\%$, see Fig. 5 top. Biases are closer to zero for higher thresholds, since the corresponding probabilities are smaller. Several reasons causing these occasional biases are conceivable. On the one hand, radar measurements are susceptible to interference that can result in systematic errors for some regions. On the other hand, we indicated in [8], where a verification of area probabilities for the occurrence of precipitation covering the same period is performed, that biases in estimated area probabilities are induced by biases in the underlying point probabilities (even if these are smaller). Indeed, we observe positive biases of point and area probabilities in northern Germany and small negative biases in southern Germany. Thus, it seems that biases of estimated area probabilities are caused (and slightly amplified) by the underlying point probabilities.

At next, Brier skill scores and empirical correlation coefficients are analyzed. In general, these scores decrease with increasing threshold (for both point and area probabilities), which shows that precipitation events occurring less frequently are more difficult to predict. We find that averaged scores as well as almost all single scores are clearly positive for all thresholds up to $u = 3$ mm, see Fig. 5 center and bottom. Furthermore, a direct comparison with the scores computed from the underlying point probabilities, see Fig. 4 center and bottom, shows that Brier skill scores and correlation coefficients of estimated area probabilities for thresholds up to 2 mm actually perform slightly better than the corresponding scores of point probabilities. Even the few weather stations with more unreliable point probabilities, indicated by very low (or negative) Brier skill scores and correlation coefficients, do not affect estimated area probabilities very much. This is a particularly nice result. Again, we observe that best results (i.e., highest Brier skill scores and correlation coefficients) are obtained in those regions where the underlying data are the most reliable (i.e., have the highest Brier skill scores and correlation coefficients), whereas small insufficiencies in our method seem to be influenced by less reliable data. A meaningful verification of area probabilities estimated for thresholds of 5 mm or higher is difficult since the corresponding (extreme) precipitation events occur rarely in the data. For example, a verification of area probabilities is only possible for 34 Voronoi cells if the threshold is 10 mm and for only 1 Voronoi cell if the threshold is 15 mm. Brier skill scores and correlation coefficients are significantly smaller than for lower thresholds but still positive for most test areas. Although our results indicate that our procedure gives more reliable area probabilities for extreme precipitation events than the climate mean, we also observe that forecast quality is considerably lower than for smaller thresholds. Thus, such area probabilities should be handled with some caution.

The previously computed scores are only able to assess forecast quality in dependence of a chosen threshold. To conclude forecast verification we thus consider a score which assesses the overall forecast quality of the proposed method. For that purpose, we analyze the ranked probability skill score, see e.g. [2] or [20]. This score can be considered as a multiple-category version of the Brier skill score and is constructed as follows. At first, the interval $[0, \infty)$ of all possible precipitation amounts in mm is divided into a sequence $J_1 = [0, 0.1], J_2 = (0.1, 0.2], \dots, J_{11} = (10, 15], J_{12} = (15, \infty)$ of 12 subintervals, whose endpoints correspond to the thresholds considered above. Then, for each forecast period and Voronoi cell we determine sequences $y_1, \dots, y_{12}$ and $o_1, \dots, o_{12}$, where y_i denotes

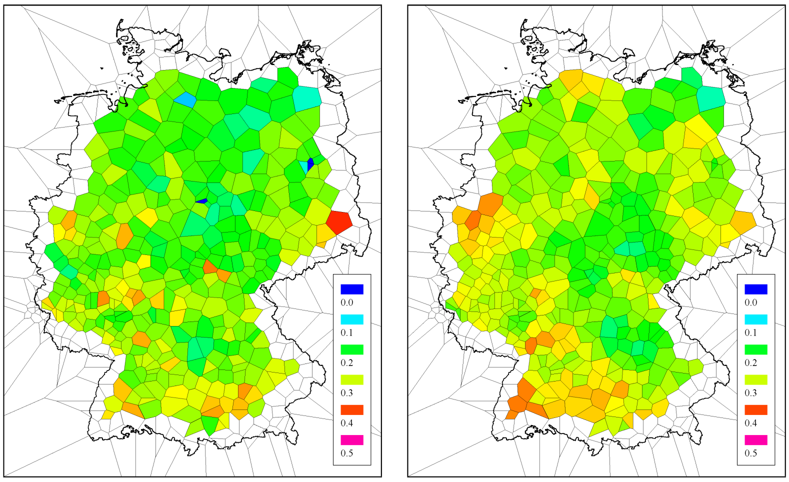

Fig. 6 Forecast verification using radar data: ranked probability skill scores for point probabilities (obtained by fitting gamma distributions to data provided by DWD; left) and area probabilities (estimated based on the proposed precipitation model; right). Voronoi cells inside the boundaries of Germany are colored according to the ranked probability skill scores of the corresponding weather stations/Voronoi cells.

the probability of a precipitation amount in J_i occurring within the considered Voronoi cell (estimated according to our method) and o_i is equal to 1 if a precipitation amount in J_i is observed according to radar data and 0 otherwise for $i = 1, \ldots, 12$. Then, the ranked probability score RPS is computed as

$$RPS = \sum_{m=1}^{12} \left(\left(\sum_{i=1}^{m} y_i \right) - \left(\sum_{i=1}^{m} o_i \right) \right)^2 . \tag{14}$$

Similar as for the Brier skill score a reference rank probability score $\widetilde{RPS}$ is computed based on the climate mean and the ranked probability skill score is determined as $1 - RPS/\widetilde{RPS}$. Analogously, ranked probability skill scores can be computed for the underlying point probabilities. Values of this score should be positive and as high as possible. Fig. 6 shows the ranked probability skill scores of all weather stations and Voronoi cells inside the boundaries of Germany. All computed values (except for three stations) are clearly positive with values between 0.15 and 0.4. In particular, we find that scores for area probabilities have similar values as those for point probabilities, which indicates that our method provides forecasts that have a similar quality as the underlying data. The mean ranked probability score of area probabilities even has a higher value than that for point probabilities (point probabilities: 0.25, area probabilities: 0.28). We conclude that precipitation events occur mainly in those areas and forecast periods, where the corresponding estimated area probabilities are high.

7 Conclusion

In the present paper we extended a stochastic modeling approach for the computation of area precipitation probabilities, which was recently introduced in [8]. For the first time, a combined model for precipitation cells and precipitation amounts is given, which allows for the estimation of area probabilities for the occurrence of precipitation exceeding arbitrary thresholds while fulfilling requirements for application in operational weather prediction. In the proposed model, precipitation cells are represented by a non-stationary germ-grain model with circular grains described by a sequence of random local intensities and a random grain radius. A randomly scaled response function is assigned to each precipitation cell and the summed response functions are interpreted as random precipitation amounts. Most model characteristics, i.e., intensities of precipitation cells, cell radius and expectations and variances of random scaling variables, were computed for each forecast period separately based on point probabilities for the occurrence of precipitation exceeding different thresholds. In particular, all characteristics are determined algorithmically based on predicted point probabilities, i.e., no precipitation observations are needed for model fitting. Since no further input of the forecaster is necessary and due to the reasonable computation time, the method is suitable for the issuing of automated weather predictions and warnings on a nation-wide scale.

A comparison of estimated area probabilities with precipitation indicators obtained from radar data showed a very good agreement. For thresholds up to 3 mm we received reasonable Brier skill scores and correlation coefficients for almost all test areas (in many cases even higher than for underlying point probabilities). Biases were close to zero for most areas but also showed some deviations occasionally. Although we described possible reasons causing these biases, a higher precision of estimated probabilities will be a goal of future work. For higher thresholds (5 mm or more) forecast verification shows less significant results. It seems that area probabilities are slightly underestimated and forecast quality is lower than for smaller thresholds. Nevertheless, we obtained positive Brier skill scores and correlation coefficients for most test areas indicating that predicted probabilities are superior to naive estimators as the climate mean. The analysis of ranked probability skill scores also reveals a clear relationship between estimated area probabilities and radar observations. Here, we get similar values for point and area probabilities, too, which indicates that forecasts provided by the proposed method have a similar quality as the underlying data. On the other hand, however, we observe that the considered verification scores for area probabilities correspond strongly to the scores of underlying point probabilities. Thus, precise and unbiased data are crucial for the success of the presented method. Although it is not completely clear whether the lower quality of area probabilities for extreme thresholds is caused by the underlying data or the method, we will consider the computation of more precise area probabilities for extreme precipitation events as one major goal in future research. It also needs to be investigated how the presented approach works for areas with sizes and shapes varying from those investigated here or in regions with different climatological or geographical conditions than central Europe.

The proposed methodology is not only expected to further sensitize the meteorological community for the difference of point and area probabilities and thus will strengthen the consideration of area probabilities (for different weather events) in probabilistic weather prediction. Additionally, the proposed precipitation model can also be used to estimate further characteristics that might be interesting for the issuing of weather warnings (and do not necessarily depend on extreme precipitation events). For example, it is possible to estimate the mean cumulated precipitation amount that occurs in an area, e.g. the drainage area of a river, over a longer time period to assess flood risks. Such applications, however, are beyond the scope of the present paper and could be a topic of future research. Furthermore, this kind of models can be applied to other weather events, e.g., the occurrence of wind gusts or thunderstorms exceeding a certain strength. However, it is crucial that the size of "cells" in the considered weather event is not too small in comparison to the density of weather stations.

Appendix

We give a brief derivation of equations (6) and (7) for the conditional expectation and variance of the random precipitation amount Γ_t at $t \in W$ given $\{E = e\}$. In order to derive (7), we need the following general result for Poisson processes. Let $\{Y_i, i = 1, 2, \ldots\}$ be a Poisson process in $\mathbb{R}^2$ with locally integrable intensity function $\lambda : \mathbb{R}^2 \to [0, \infty)$, second-order moment measure $\mu^{(2)} : \mathcal{B}(\mathbb{R}^2 \times \mathbb{R}^2) \to [0, \infty]$ and second-order product density $\varrho^{(2)} : \mathbb{R}^2 \times \mathbb{R}^2 \to [0, \infty)$. Furthermore, let $f, g : \mathbb{R}^2 \to [0, \infty)$ be two nonnegative measurable functions. By using the definition of the second-order moment measure and the result that $\varrho^{(2)}(x, y) = \lambda(x)\lambda(y)$ for $x, y \in \mathbb{R}^2$, see e.g. [4], p. 119, we get

$$
\begin{aligned}
\mathbb{E}\left(\sum_{i=1}^{\infty} f(Y_i) \sum_{j=1}^{\infty} g(Y_j)\right) &= \mathbb{E}\left(\sum_{i,j=1}^{\infty} f(Y_i)\, g(Y_j)\right) \\
&= \int\int f(x)\, g(y)\, \mu^{(2)}(\mathrm{d}(x, y)) \\
&= \int\int f(x)\, g(y)\, \varrho^{(2)}(x, y)\, \mathrm{d}(x, y) + \int f(x)\, g(x)\, \lambda(x)\, \mathrm{d}x \\
&= \int f(x)\, \lambda(x)\, \mathrm{d}x \int g(y)\, \lambda(y)\, \mathrm{d}y + \int f(x)\, g(x)\, \lambda(x)\, \mathrm{d}x.
\end{aligned}
$$

We start with equation (6) for the conditional expectation $\mathbb{E}(\Gamma_t \,|\, E = e)$ of Γ_t given $\{E = e\}$. In the following, we again use the notation introduced in Sect. 4, i.e., let $a_j = \mathbb{E}(A_j \,|\, E = e)$, $c_j = \mathbb{E}(C_j \,|\, E = e)$ and $\tilde{c}_j = \mathrm{var}(C_j \,|\, E = e)$ for $j = 1, \ldots, n$ and $r = \mathbb{E}(R \,|\, E = e)$. Recall that conditioned on $\{E = e\}$ the point process $\{X_i, i = 1, \ldots, Z\}$ is a Poisson process with intensity function $\{\lambda_t, t \in W\}$, where $\lambda_t = \sum_{j=1}^{n} a_j I_{V(s_j)}(t)$ for all $t \in W$. Furthermore, $\{X_i, i = 1, \ldots, Z\}$ is conditionally independent of the scaling variables $C_1, \ldots, C_n$ given $\{E = e\}$. By applying the Campbell theorem for point processes (see e.g. [1], Theorem 4.1) we get

$$
\begin{aligned}
\mathbb{E}(\Gamma_t \,|\, E=e) &= \mathbb{E}\left(\sum_{i=1}^{Z}\sum_{j=1}^{n} C_j I_{V(s_j)}(X_i) K_p(t, X_i, R) \,\Big|\, E=e\right) \\
&= \sum_{j=1}^{n} c_j\, \mathbb{E}\left(\sum_{i=1}^{Z} I_{V(s_j)}(X_i) K_p(t, X_i, r) \,\Big|\, E=e\right) \\
&= \sum_{j=1}^{n} c_j \int I_{V(s_j)}(x) \left(1-\frac{|t-x|^2}{r^2}\right)^p I_{b(t,r)}(x) \sum_{k=1}^{n} a_k I_{V(s_k)}(x)\,\mathrm{d}x \\
&= \sum_{j=1}^{n} \mathbb{E}(C_j \,|\, E=e)\; a_j \int_{V(s_j)\cap b(t,r)} \left(1-\frac{|t-x|^2}{r^2}\right)^p \mathrm{d}x.
\end{aligned}
$$

Now, we consider the conditional variance $\mathrm{var}(\Gamma_t \,|\, E=e)$ for a fixed $t \in W$. To simplify the notation we introduce the function $f_j : \mathbb{R}^2 \to [0,\infty)$ with $f_j(x) = I_{V(s_j)}(x) K_p(t,x,r)$ for all $x \in \mathbb{R}^2$ and $j = 1,\ldots,n$. Obviously, $f_j(x) f_k(x) = 0$ for all $x \in \mathbb{R}^2$ if $j \neq k$. Furthermore, $\int f_j(x)\,\mathrm{d}x = I(s_j,t)$ and $\int f_j^2(x)\,\mathrm{d}x = \tilde{I}(s_j,t)$ for $j = 1,\ldots,n$, where $I(s_j,t)$ and $\tilde{I}(s_j,t)$ are defined according to equations (8) and (9). By using the result for Poisson processes shown before and that conditioned on $\{E=e\}$, the scaling variables $C_1,\ldots,C_n$ are independent of each other and of $\{X_i, i=1,\ldots,Z\}$, we get that

$$
\begin{aligned}
&\mathbb{E}\left(\Gamma_t^2 \,\Big|\, E=e\right) = \mathbb{E}\left(\left(\sum_{i=1}^{Z}\sum_{j=1}^{n} C_j I_{V(s_j)}(X_i) K_p(t,X_i,R)\right)^2 \,\Big|\, E=e\right) \\
&= \mathbb{E}\left(\sum_{j=1}^{n}\sum_{k=1}^{n} C_j C_k \sum_{i=1}^{Z} I_{V(s_j)}(X_i) K_p(t,X_i,R) \sum_{l=1}^{Z} I_{V(s_k)}(X_l) K_p(t,X_l,R) \,\Big|\, E=e\right) \\
&= \sum_{j=1}^{n}\sum_{k=1}^{n} \mathbb{E}(C_j C_k \,|\, E=e)\, \mathbb{E}\left(\sum_{i=1}^{Z} f_j(X_i) \sum_{l=1}^{Z} f_k(X_l) \,\Big|\, E=e\right) \\
&= \sum_{j=1}^{n}\sum_{k=1}^{n} \mathbb{E}(C_j C_k \,|\, E=e) \left(\int f_j(x)\, a_j\,\mathrm{d}x \int f_k(x)\, a_k\,\mathrm{d}x + \int f_j(x)\, f_k(x)\, \lambda_x\,\mathrm{d}x\right) \\
&= \sum_{j=1}^{n} \mathbb{E}(C_j^2 \,|\, E=e) \left(a_j^2\, I^2(s_j,t) + a_j\, \tilde{I}(s_j,t)\right) + \sum_{j=1}^{n}\sum_{\substack{k=1\\k\neq j}}^{n} c_j\, c_k\, a_j\, a_k\, I(s_j,t)\, I(s_k,t).
\end{aligned}
$$

Moreover, according to equation (6), we get

$$\begin{aligned}\big(\mathbb{E}\,(\Gamma_t \mid E = e)\big)^2 &= \left(\sum_{j=1}^{n} c_j\, a_j \int_{V(s_j)\cap b(t,r)} \left(1 - \frac{|t-x|^2}{r^2}\right)^p \mathrm{d}x\right)^2 \\ &= \sum_{j=1}^{n}\sum_{k=1}^{n} c_j\, c_k\, a_j\, a_k\, I(s_j,t)\, I(s_k,t) \\ &= \sum_{j=1}^{n} c_j^2\, a_j^2\, I^2(s_j,t) + \sum_{j=1}^{n}\sum_{\substack{k=1\\k\neq j}}^{n} c_j\, c_k\, a_j\, a_k\, I(s_j,t)\, I(s_k,t).\end{aligned}$$

Finally, combining both representation formulas results in

$$\begin{aligned}\mathrm{var}(\Gamma_t \mid E = e) &= \mathbb{E}\left(\Gamma_t^2 \,\middle|\, E = e\right) - \big(\mathbb{E}\,(\Gamma_t \mid E = e)\big)^2 \\ &= \sum_{j=1}^{n} \mathbb{E}(C_j^2 \mid E = e)\left(a_j^2\, I^2(s_j,t) + a_j\, \tilde{I}(s_j,t)\right) - \sum_{j=1}^{n} c_j^2\, a_j^2\, I^2(s_j,t) \\ &= \sum_{j=1}^{n} \tilde{c}_j \left[a_j \tilde{I}(s_j,t) + a_j^2 I^2(s_j,t)\right] + \sum_{j=1}^{n} c_j^2 a_j \tilde{I}(s_j,t),\end{aligned}$$

which coincides with the representation formula for the conditional variance of Γ_t given in (7).

References

1. Chiu, S.N., Stoyan, D., Kendall, W.S., Mecke, J.: Stochastic Geometry and its Applications, 3rd edn. J. Wiley & Sons, Chichester (2013)
2. Daan, H.: Sensitivity of verification scores to the classification of the predictand. Mon. Weather Rev. **113**, 1384–1392 (1985)
3. Epstein, S.E.: Point and area precipitation probabilites. Mon. Weather Rev. **94-10**, 595–598 (1966)
4. Illian, J., Penttinen, A., Stoyan, H., Stoyan, D.: Statistical Analysis and Modelling of Spatial Point Patterns. J. Wiley & Sons, Chichester (2008)
5. Jacod, J., Protter, P.E.: Probability Essentials, 2nd edn. Springer, Berlin (2004)
6. Knüpffer, K.: Methodical and predictability aspects of MOS systems. In: 13th Conf. on Probability and Statistics in Atmosph. Sciences, pp. 190–197. Amer. Meteorol. Soc., San Francisco, CA (1996)
7. Koubek, A., Pawlas, Z., Brereton, T., Kriesche, B., Schmidt, V.: Testing the random field model hypothesis for random marked closed sets. Spat. Stat. **16**, 118–136 (2016)
8. Kriesche, B., Hess, R., Reichert, B.K., Schmidt, V.: A probabilistic approach to the prediction of area weather events, applied to precipitation. Spat. Stat. **12**, 15–30 (2015)
9. Kriesche, B., Koubek, A., Pawlas, Z., Beneš, V., Hess, R., Schmidt, V.: A model-based approach to the computation of area probabilities for precipitation exceeding a certain threshold. In: Proceedings of the 21st International Congress on Modelling and Simulation, pp. 2103–2109. Modelling and Simulation Society of Australia and New Zealand, Gold Coast (2015)
10. Krzysztofowicz, R.: Point-to-area rescaling of probabilistic quantitative precipitation forecasts. J. Appl. Meteorol. **38**, 786–796 (1998)
11. Lanza, L.G.: A conditional simulation model of intermittent rain fields. Hydrol. Earth Syst. Sci. **4**(1), 173–183 (2000)
12. Lawson, C.L., Hanson, R.J.: Solving Least Squares Problems. Prentice-Hall, Englewood Cliffs, NJ (1974)

13. Majewski, D., Liermann, D., Prohl, P., Ritter, B., Buchhold, M., Hanisch, T., Paul, G., Wergen, W., Baumgardner, J.: The global icosahedral-hexagonal grid point model GME: description and high-resolution tests. Mon. Weather Rev. **130**(2), 319–338 (2002)
14. Mayer, J., Schmidt, V., Schweiggert, F.: A unified simulation framework for spatial stochastic models. Simul. Model. Pract. Theory **12**(5), 307–326 (2004)
15. Onof, C.J., Chandler, R.E., Kakou, A., Northrop, P.J., Wheater, H.S., Isham, V.S.: Rainfall modelling using Poisson-cluster processes: a review of developments. Stoch. Environ. Res. Risk Assess. **14**(6), 384–411 (2000)
16. Rodriguez-Iturbe, I., Cox, D.R., Eagleson, P.S.: Spatial modelling of total storm rainfall. Proc. Royal Soc. Lond. A **403**(1824), 27–50 (1986)
17. Sivapalan, M., Wood, E.F.: A multidimensional model of nonstationary space-time rainfall at the catchment scale. Water Resour. Res. **23**(7), 1289–1299 (1987)
18. Smith, J.A., Krajewski, W.F.: Statistical modeling of space-time rainfall using radar and rain gage observations. Water Resour. Res. **23**(10), 1893–1900 (1987)
19. Wheater, H.S., Chandler, R.E., Onof, C.J., Isham, V.S., Bellone, E., Yang, C., Lekkas, D., Lourmas, G., Segond, M.-L.: Spatial-temporal rainfall modelling for flood risk estimation. Stoch. Environ. Res. Risk Assess. **19**(6), 403–416 (2005)
20. Wilks, D.S.: Statistical Methods in the Atmospheric Sciences, 3rd edn. Academic Press, San Diego (1995)
21. Wilks, D.S., Eggleston, K.L.: Estimating monthly and seasonal precipitation distributions using the 30- and 90-day outlooks. J. Clim. **10**, 77–83 (1992)
22. Winterrath, T., Rosenow, W., Weigl, E.: On the DWD quantitative precipitation analysis and nowcasting system for real-time application in German flood risk management. In: R.J. Moore, S.J. Cole, A.J. Illingworth (eds.) Weather Radar and Hydrology (Proceedings of a symposium held in Exeter, UK, April 2011), vol. IAHS 351, pp. 323–329 (2012)
23. Yang, C., Chandler, R.E., Isham, V.S., Wheater, H.S.: Spatial-temporal rainfall simulation using generalized linear models. Water Resour. Res. **41** (2005)
24. Zängl, G., Reinert, D., Rípodas, P., Baldauf, M.: The ICON (ICOsahedral Non-hydrostatic) modelling framework of DWD and MPI-M: description of the non-hydrostatic dynamical core. Q. J. Royal Meteorol. Soc. **141**, 563–579 (2015)